International Journal of Applied Geospatial Research
Volume 15 • Issue 1

Automated Detection of On-Farm Irrigation Reservoirs in Two Critical Groundwater Regions of Arkansas:

A Necessary Precursor for Conjunctive Water Management

Daniel D. Shults, Arkansas State University, USA
John W. Nowlin, Arkansas State University, USA*
https://orcid.org/0000-0002-2891-028X
Joseph H. Massey, USDA-ARS, USA
Michele L. Reba, USDA-ARS, USA
https://orcid.org/0000-0001-6830-0438

ABSTRACT

In eastern Arkansas, the use of surface water for crop irrigation is steadily increasing in response to declining aquifers. Effective conjunctive water management requires accurate and timely information on the locations, sizes, and numbers of on-farm irrigation reservoirs. A method for remotely locating and characterizing on-farm reservoirs was developed using relative elevation and near-infrared imagery. With 62% accuracy, the method automatically identified 429 irrigation reservoirs within a 1.9-Mha area in less than an hour using an off-the-shelf laptop. Reservoirs not accurately identified (i.e., false negatives) were caused by the presence of vegetation or turbidity within the reservoirs. There were no false positive detections. This approach for identifying elevated reservoirs is applicable across the Mississippi Alluvial Plain (MAP) that encompasses over 4-Mha of irrigated cropland and other agricultural areas having low-relief.

KEYWORDS

ArcGIS Pro Model Builder, Automated Reservoir Detection, Conjunctive Water Management, Topographic Modeling, Waterbody Classification

INTRODUCTION

The Mississippi River Valley Alluvial Aquifer (MRVAA) provides 90% of the irrigation water applied to crops in the Mississippi Alluvial Plain (MAP) (Leslie et al., 2022). The aquifer has been over-exploited for decades (Bedinger et al., 1964; Clark et al., 2011; 2013; Vories & Evett, 2014). In order to capture precipitation/runoff and reduce groundwater withdrawals, irrigation reservoirs are being

DOI: 10.4018/IJAGR.337287 *Corresponding Author

constructed on farms throughout the MAP (Evett et al., 2003). Additionally, in central Arkansas, two large surface water diversion projects will use on-farm reservoirs to store water removed from the White River and the Arkansas River to offset groundwater pumping (USACE, 1999; 2007).

These on-farm reservoirs can be stand-alone structures or may be part of more complex systems having a tailwater recovery 'pit' or 'ditch' to capture runoff (Figure 1). In both cases, the reservoirs are generally symmetrical (e.g., square, rectangular, triangular), relatively compact (i.e., small perimeter-to-surface area ratio), and surrounded by raised earthen levees (Yaeger et al., 2018).

Strategies to conjunctively manage surface and ground water resources (Kovacs et al., 2016; Singh et al., 2016) have been adopted in Arkansas (ANRC, 2014; 2016; 2017; 2019), Mississippi (YMD, 2006), Louisiana (E&E INC, 2011), and Missouri (MDNR, 2020). As a result, accurate and up-to-date information on irrigation reservoirs is necessary to allow resource managers and policymakers to (a) assess how existing reservoirs may impact groundwater demand, (b) determine where surface waters could support additional reservoir(s), (c) estimate maintenance costs and life expectancies of existing reservoir infrastructure, and (d) determine carrying capacity of reservoir area per watershed area.

Figure 1 shows examples of (A) two on-farm irrigation reservoirs in Eastern Arkansas that receive water pumped from streams and/or a tailwater recovery ditch (center) and (B) corresponding elevation profile. Note the western reservoir's high turbidity in contrast to the eastern reservoir.

The construction of reservoirs in the MAP may occur solely at the expense of farmers and/or landowners but more commonly occurs with assistance from federal and state agencies (Czarnecki et al., 2024; King, 2021). In Arkansas, approximately $45 million were awarded by the USDA Natural

Figure 1. Irrigation reservoirs in eastern arkansas and their corresponding elevation profiles

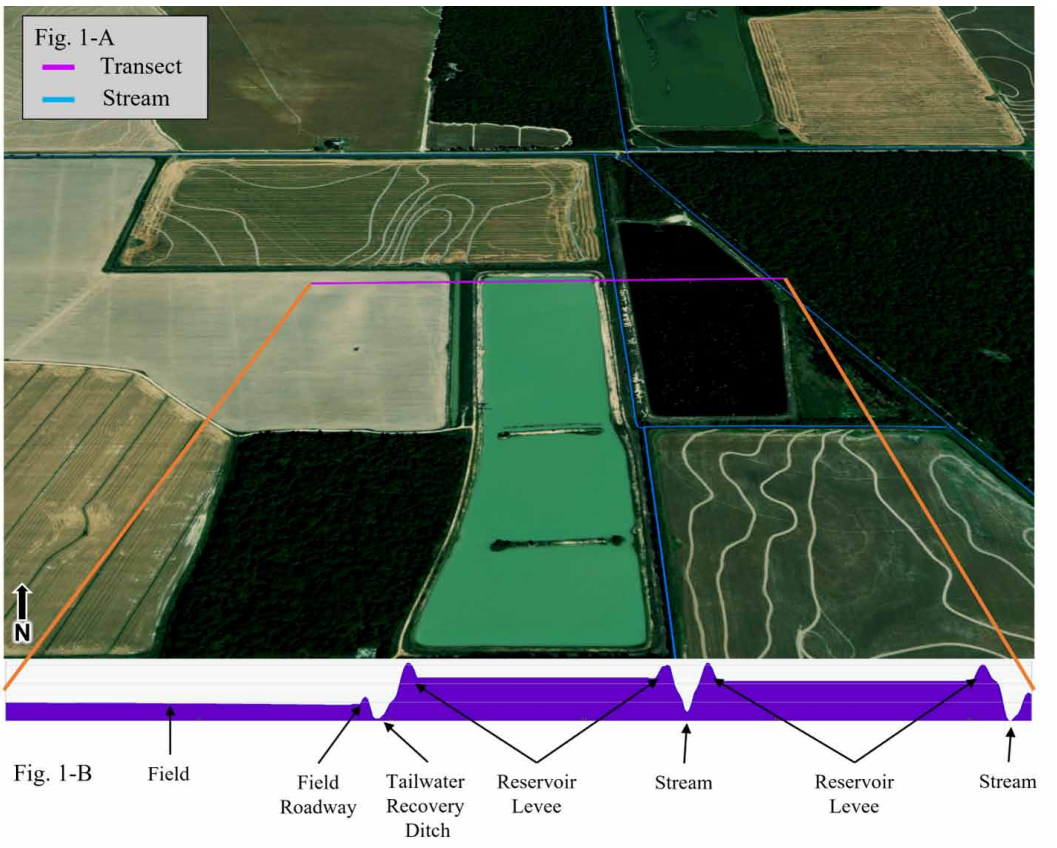

Resources Conservation Service (NRCS) between 2004 and 2018 for reservoir, tailwater recovery, and related construction (King, 2021; USDA-NRCS, 2019). The locations of reservoirs recently constructed using public funds are generally known to state and federal personnel, but this is not necessarily true for older reservoirs and/or those constructed using private funds. Thus, reservoir locations, sizes, and construction dates are difficult to determine for a region as vast and dynamic as the MAP.

While it had been decades since the earliest reservoirs were constructed, the numbers and sizes of irrigation reservoirs in Arkansas were not available until Yaeger et al. (2017) conducted comprehensive inventories for the Grand Prairie Critical Groundwater Area (GPCGA) and Cache River Critical Groundwater Area (CRCGA). The authors used three-band National Agriculture Imagery Program (NAIP) imagery (USDA-FSA, 2011) to visually identify 143 on-farm reservoirs in the nearly 0.9-Mha CRCGA and 632 reservoirs in the approximately 1-Mha GPCGA. Their goal was to perform a census, and their method of image interpretation relied on expert knowledge and visual identification based on their familiarity with the reservoirs in eastern Arkansas. When a reservoir was found, the boundary was then delineated by manually defining the boundary by hand using the editing tools in the Environmental Systems Research Institute (ESRI) ArcMap mapping software. The reservoir polygons were in the form of vector polygon features. This inventory took many months to perform, not only because of ground truthing, but also because of the large area and the heterogeneous characteristics of the bodies of water used as irrigation reservoirs. Unfortunately, given the dynamic nature of the MAP, these data are already dated. Moreover, the visual methods used are time-consuming and, thus, do not lend themselves to timely inventories needed by landowners, water planners, policymakers, modelers, and other stakeholders.

There are multiple authoritative datasets that reference waterbodies in the MAP, including the National Land Cover Dataset, the Cropland Data Layer (CDL), and the National Hydrography Dataset (NHD). Unfortunately, these datasets do not differentiate between irrigation reservoirs and many other common waterbodies such as aquacultural ponds, ditches, canals, lakes, borrow pits, settling basins, etc. Also, the nature of the high rate of landform modifications for irrigation management in this actively managed agricultural landscape and the ephemeral waterbodies (flooding of fields both for agriculture and waterfowl) complicates the classification of waterbodies in such regions. Furthermore, such high rates of change render many such datasets out-of-date in a matter of years. Currently, there is not an efficient method for differentiating between irrigation reservoirs and other bodies of water using remotely sensed data.

Multi-spectral imagery has long been used to differentiate water from land (Gao, 1996). More recently, multi-spectral imagery was used to create deep-learning algorithms to classify irrigation systems (Raei et al., 2022). The delineation of natural water features in alluvial settings with satellite imagery has been successfully accomplished (Frazier & Page, 2000; Alexandridis et al., 2008). In dry environments where reservoirs are easily differentiated from natural water features, remote sensing has proven useful in estimating reservoir volume, but it requires manual surveying to estimate reservoir depth (Rodrigues et al., 2012). Satellite imagery has been useful for automated mapping of flooded agriculture like paddy rice (Zhang et al., 2021). Flooded rice agricultural landscapes—as a landcover type—are unique in that paddies are bounded by levees, and water is obscured by rice after canopy closure. Also, the fields may be flooded in the off season, making the differentiation of a field from a reservoir difficult with imagery alone.

One difficult problem for remote sensing of irrigation reservoirs is differentiating reservoirs from natural water features. Digital elevation models (DEMs) are often used in hydrologic modeling, such as in delineating streams, a process tailored to geographic information systems (GISs) (DeVantier & Feldman, 1993; Preusch & Rezakhani, 1999). DEMs are also useful in the design and quantification of reservoir volume (Masharif & Khasanov, 2021). Wu et al. (2019) integrated elevation surfaces with aerial imagery to find lakes and the boundaries of their respective depressions. They identified water using an unsupervised classification of NAIP imagery using both the Normalized Difference Water Index (NDWI) (McFeeters, 1996) and the Normalized Difference Vegetation Index (NDVI)

(Tucker, 1979) to model the ephemeral shorelines of the natural bodies of water in a region of lakes in Minnesota. Then, to model wetland inundation, they incorporated remote sensing method, Light Detection and Ranging (LiDAR). Thus, LiDAR-based elevation surfaces were used to estimate the maximum extents of the wetlands.

The near infrared (NIR) threshold technique for classifying water is a method involving a single band. When classifying land cover with RapidEye satellite imagery in Eti-Osa (a sub-region of Lagos, Nigeria), Mondejar and Tongco (2019) found the NIR threshold outperformed other indices like the NDWI, the modified normalized difference water index (MNDWI), and one of two automated water extraction indexes (AWEIs) (Feyisa et al., 2014). It is notable that this means of finding water is simpler than indices involving multiple bands.

GIS and remote sensing are often used in conjunction to solve spatial problems; for example, Khan et al. (2022) studied historical flood data in flood hazard zones in the Budhni Nullah District Peshawar, Pakistan. They used Landsat satellite imagery and qualitative data collected by local sources to learn the causes of the flooding, determine where damage occurred, and delineate the flood zones along rivers in the region. They used a variety of programs including statistical data analysis software, Statistical Package for the Social Sciences (SPSS) for statistical quantification; Earth Resources Development Assessment System (ERDAS) Imagine, remote sensing image processing software for image processing; a global positioning system (GPS) application for in-situ collection of location; and a variety of ESRI ArcGIS Spatial Analyst tools for hydrological modeling.

LiDAR-based elevation surfaces and aerial imagery have also been integrated to find damage to flood levees along the Vistula River in Annopol, Poland (Bakuła et al., 2020). These structures are similar to the levees around raised, on-farm reservoirs, albeit they are used for flood control instead of irrigation water storage. Another study related to river flooding used DEMs to characterize floodplains along the Opava River in the Czech Republic. One notable aspect of this study was the use of the ArcGIS's ModelBuilder tool to string together multiple geoprocessing tools in order to "perform the whole delineation process automatically after setting several input parameters" (Hartvich & Jedlička, 2019).

The Problem

The problem we are highlighting is the need to update and maintain a list of regional irrigation reservoirs in the Mississippi Alluvial Plain (MAP). The singular inventory of reservoirs produced by Yaeger et al. (2017), while excellent in quality, is aging. Many new reservoirs have been established, and existing reservoirs have been modified since the inventory was conducted. To effectively manage water in the region, this inventory needs updating again.

The Aim: A New Solution

The methods used to generate this inventory were time consuming and high-effort, requiring expert regional knowledge of existing reservoirs, image interpretation conducted via manual review of aerial imagery, and manual delineation of irrigation reservoir boundaries using ESRI's ArcMap mapping software. Our conjecture was that by using the same multi-spectral imagery, NAIP, and DEMs, we could construct a GIS model to automatically differentiate on-farm reservoirs from natural bodies of water and produce a set of polygons for these reservoirs faster than Yaeger et al. (2017) using ArcGIS Pro. Such a model could then be used to regularly update and maintain an authoritative database of irrigation reservoirs for use in planning and conjunctive management of water resources. Optimally, such a tool would be usable with different spatial resolutions and data sources and would be useful to others outside our region but with similar low relief settings like alluvial or coastal plains.

Objectives

Our aim was to create an automated method for identification of on-farm reservoirs in northeast Arkansas. Specific objectives were to: (1) develop a model using ArcGIS Pro ModelBuilder that

can identify the locations and surface areas of on-farm irrigation reservoirs, (2) assess the accuracy of the model by comparison with the Yeager (2017) on-farm reservoir dataset, (3) record the raised status of the existing on-farm reservoir dataset, and (4) generate an updated inventory of on-farm reservoirs. Furthermore, we wanted to compare the on-farm reservoir inventory with water features from the National Hydrography Database (NHD) and water classes from Cropland Data Layer (CDL) to determine their usefulness in identifying on-farm reservoirs as waterbodies.

MATERIALS AND METHODS

Study Area

The study area is comprised of three contiguous regions of intensive agricultural production in northeastern Arkansas which itself lies within the MAP (Figure 2). The regions consist of the GPCGA, the CRCGA, and a non-critical groundwater area (CGA) representing the remaining portion of the MAP north of the GPCGA and west of the CRCGA (ANRC, 2019). Together, these three zones comprise a 2.3-Mha region immediately west and southwest of Crowley's Ridge (Figure 2). Even though the watershed receives an average annual precipitation of approximately 1,000 mm, irrigation water availability is still a concern (Kresse et al., 2014). The MRVAA shows two significant cones of depression, one in the GPCGA and another in the CRCGA (Figure 2).

Figure 2. Map of the cones of depression in the MRVAA intersecting the CRCGA, GPCGA and Non-CGA boundaries

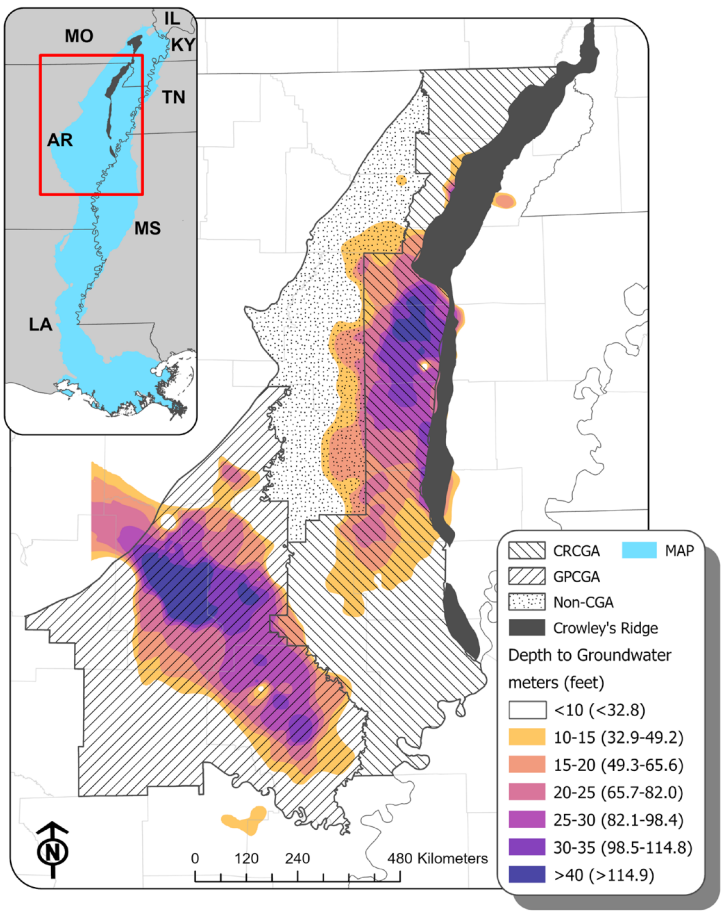

Figure 2 depicts the GPCGA and CRCGA range from central to eastern Arkansas within the MAP that lay atop two cones of depression formed in the Mississippi River Valley alluvial aquifer MRVAA. The depth-to-water estimates are from 2020 (USGS, 2020).

Model Development

A model with seven sub-routines was constructed in ArcGIS Pro (V. ≥ 2.7.3 with the Spatial Analyst Extension; ESRI, Redlands, CA).

The model requires high spatial resolution (< 1- to 3-meter) input data, including: four-band aerial imagery (near-infrared, red, green, and blue), and a DEM with a spatial resolution of 1 m. It is expected that higher resolutions (≤ 1 m) for the imagery and DEM will produce more refined results, but lower resolutions (3-5 m) should provide meaningful results too. Thus, the model's design makes it capable of being used with a wide range of datasets making it useful outside the study area and specific datasets presented in this project.

Four-band NAIP imagery from 2019 was used for its high resolution, NIR band capability, and bi-annual collection. For the DEM, the most recent available LiDAR-based, one-meter DEM (USDA-FSA, 2019; USGS, 2011) was used. This tool was run using an off-the-shelf laptop (Dell Inc., Round Rock, TX, 78664; Model XPS 17, Intel Core i9-10885H CPU @ 2.40 GHz, 64GB RAM, 2TB SSD).

Initially, we intended to use the NDWI method of detecting water using multi-band aerial imagery (Gao, 1996). In our trial-and-error testing with NAIP imagery, while preparing the bands, we noticed that the NIR band alone was a good predictor for water. Therefore, we decided to include both methods in the model, so we could compare the results independently. The first process in the model reflects these two paths, described as the "NIR only" iteration and the "NDWI" iteration, respectively. The results for each iteration are reported separately in Table 3.

Equation (1) shows that the NDWI utilizes the green band and the NIR band.

$$NDWI = \frac{Green - NIR}{Green + NIR} \tag{1}$$

In both iterations of this step, four-band imagery is needed (Figure 3A), from which the NIR band and green bands are used to identify water (Figure 3B) with two different methods. All bands of NAIP imagery have eight-bit spectral resolution ($2^8 = 256$ light levels), where the pixel value ranges from 0–255. In NAIP (2019), green is the 2nd band, and NIR is the 4th band in the dataset. Vegetation reflects green light and NIR resulting in relatively high reflectance values for vegetation in the green and NIR band. In contrast, water absorbs NIR, resulting in relatively low reflectance values for water in the NIR band.

Figure 3 represents a stepwise approach used to identify irrigation reservoirs in northeast Arkansas where (A) represents an example of a NAIP 4-band image using a 4-3-2 (NIR-Red-Green) band combination; (B) shows the NIR band displayed in 8-bit black and white where white is reflective and black is absorptive; (C) depicts land and water reclassified using an NIR reflectance threshold where Reflectance ≤15% is water; (D) shows land polygons deleted, leaving water (Blue); (E) presents a reservoir in the digital elevation model; (F) shows use of two concentric buffers to first identify if a levee surrounds a waterbody (Purple) and relative elevation of surrounding terrain (Reddish Orange); (G) presents the compactness test formula; and (H) represents how a waterbody scoring "0" on the compactness test designates as "Not-Compact" and one scoring "1" designates as "Compact."

When viewing the Yaeger et al. (2017) reservoir polygons overlaid atop the NIR band, it was observed that water was represented by low NIR values. With a short survey, we determined that the threshold for water was below NIR values of 40, which corresponds to ~15% reflectance in this band.

This method of water classification is known as the NIR threshold method and similarly outperforms other more complex methods in Mondejar and Tongco (2019). Therefore, in this "NIR

Figure 3. Stepwise approach used to identify irrigation reservoirs in northeast Arkansas

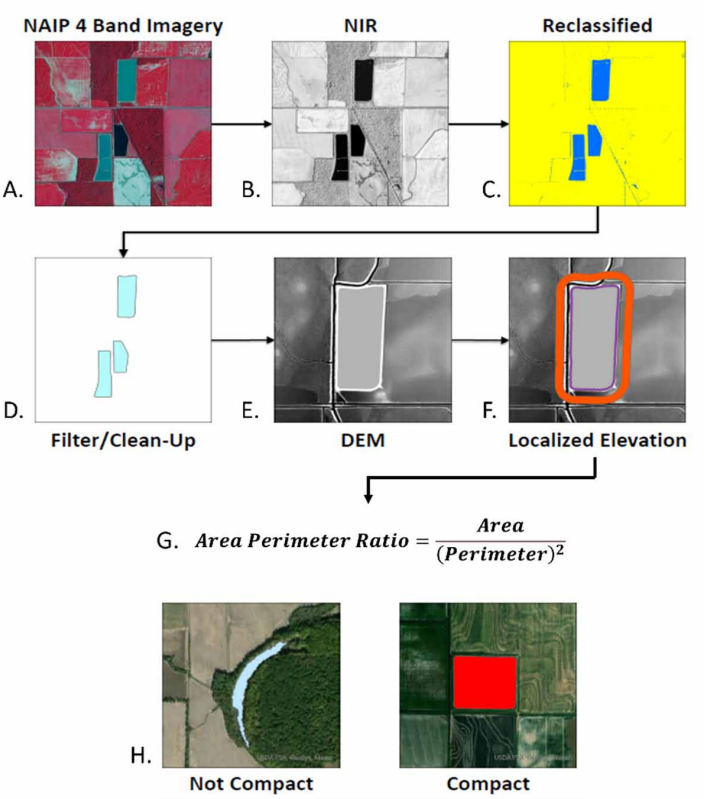

only" iteration of the model, we reclassify two classes: water (0–40) and land (41–255). If using the model with aerial imagery of another bit depth, this threshold will need to be adjusted as a calibration step, which is specific to a particular set of imagery at a particular bit depth which was collected in a particular season and place. For example, a 12-bit spectral resolution ($2^{12} = 4096$ light levels) would use a setting of 615/4096 to maintain 15% reflectance.

The NDWI outputs a floating-point raster value of 1.0 to -1.0, where the higher the number, the more likely the pixel is to be water. We classify the NDWI outputs such that the highest ~15% of this range would be classified as water, and the lower ~85% would be classified as land. This threshold is chosen to match the "NIR only" method. In numeric terms, the NDWI index output is classified as water if greater than or equal to 0.7, and land, if less than 0.7. This is somewhat higher than the 0.52 threshold referenced by Ji et al. (2009), but they are using Landsat. (Note that this threshold might need to be calibrated each time it is used in a different situation or with different data.) After each iteration above is performed, the remainder of the model is run twice, once with the NIR only output and again with the NDWI output. Based on our testing, we find the NIR output to be more useful, but the NDWI methods are saved in the model we share with the supplemental ArcGIS Pro project folder (.zip).

Following the identification of water, the raster is reclassified into water/land then vectorized into a polygon feature class (see Figure 3C). The vector format provides the attribute table which is used to store each waterbody's spatial characteristics in the following steps. The land polygons are deleted, so that the dataset is comprised of only water features. An area column (field) is added to the polygon's attribute table, and the surface area (ha) within each water feature is calculated/recorded

in this field. Waterbodies with areas below 0.4-ha in size are removed from the dataset (Figure 3D). In our trial-and-error process of choosing this threshold, we notice that this step greatly reduces the processing time because of the reduction in the number of waterbodies. This deletion also helps to reduce pixilation errors and areas where shadows or forests are misidentified as water. We also notice as we build the model that some waterbodies contain vegetation (e.g., submerged trees) and other pixilation errors. The trees and pixilation errors cause the "water features" to contain pixels that do not meet "water" criteria. Therefore, we then fill the holes in waterbody polygons and smooth the polygon's outer edges.

We analyze the area/perimeter ratio to help distinguish between compact and not-compact waterbodies (Figure 3G and 3H). Compact waterbodies are typically man-made while not-compact waterbodies often were streams, rivers, or oxbow lakes. Waterbodies with ratios greater than 0.01 are considered compact while waterbodies with ratios less than 0.01 are considered not compact (see Figure 4).

Figure 4. Histogram of waterbody area-to-perimeter (A/P) ratios

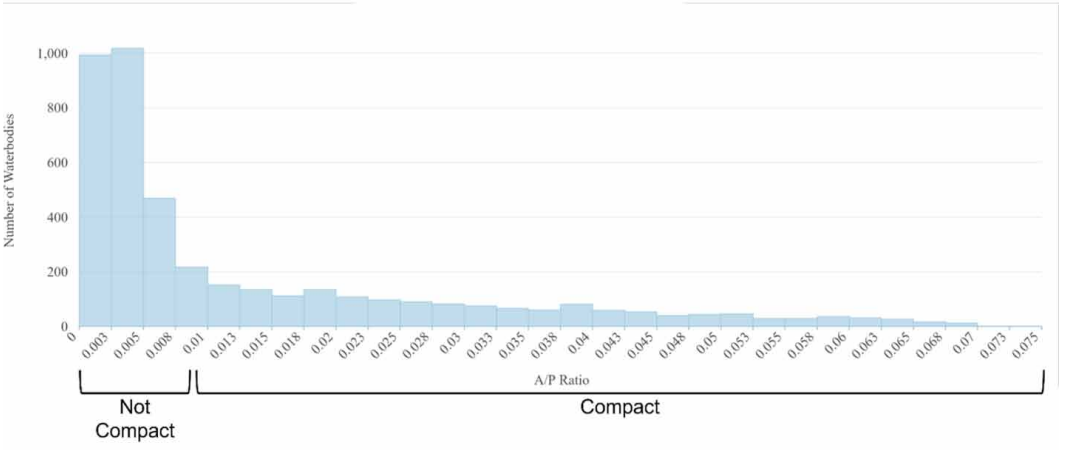

Figure 4 depicts a histogram of waterbody area-to-perimeter (A/P) ratios. Values less than 0.015 are less compact, signifying natural water features while values greater than 0.015 are more compact, signifying man-made features.

We then created buffer polygons around each compact waterbody to determine a localized elevation for each feature. Three buffers were generated at 10-m (Buffer-1), 50-m (Buffer-2), and 100-m (Buffer-3) zones respectively.

Buffer-1 is meant to contain the immediate boundary of the waterbody to essentially identify if it is surrounded by a raised, earthen levee. Buffer-2 is used as a gap to represent the engineered earthen berm outside the levee, and Buffer-3 represents the ring beyond the immediate area of the waterbody which we used to determine the elevation of the surrounding area (Figure 3F).

Using these buffer-polygons, we calculated the mean elevation of the levee (Buffer-1) and the surrounding terrain (Buffer-3). We then took the difference between these two means and recorded it for each waterbody.

An example of the results table is shared in Table 1, while the full table in the supplemental ArcGIS project folder (.zip) is shared with this article. If the difference is positive, the waterbody is raised; if the difference is negative, the waterbody is not raised. In our trial-and-error testing, we decide

to identify waterbodies raised above their surroundings by more than 1 m as irrigation reservoirs. Because soil excavated in digging a reservoir is used to construct earthen levees that surround the reservoir, this categorization is intended to differentiate on-farm irrigation reservoirs from "borrow" pits, low-lying aquaculture ponds, and other waterbodies not surrounded by levees.

It should be noted that a person standing beside a farm reservoir would often perceive the relative height of its levees as being greater than 1 m. However, when evaluating the reservoir in relation to its position in the broader landscape, which contains ditches, roads, and cultivated area, 1 m is determined to be a reasonable threshold (Figure 2-B). In our initial testing, the 1-m criteria prove to be the most accurate during model validation, but many reservoirs fall under this threshold. Therefore, we group waterbodies into four classes by compactness and levee height. The waterbody classes are summarized in Table 2. Examples of these types can be seen in Figure 6.

Table 1 indicates an example of the mean statistics calculated for each zone of the waterbody showing how relative elevation in landscape was used to differentiate irrigation reservoirs from other man-made structures in the Arkansas portion of the Mississippi Alluvial Plain. The full table in the supplemental ArcGIS project folder (.zip) is shared with this article.

Table 1. Example comparison of mean elevation in buffer zones determining if the waterbodies are raised

Waterbody Feature ID	Elevation of Levee (10 m Buffer)	Elevation of Terrain (50 - 100 m Buffer)	Mean Elevation Difference (m)
1	98.91	95.56	3.35
2	127.70	123.27	4.43
3	89.51	85.29	4.22
4	77.92	74.37	3.56
n	…	…	…

Table 2. Waterbody classification criteria

Waterbody Classification Criteria	Class
Not Compact	Null
Not Raised	0
0 < Raised < 1 m	1
Raised > 1 m	2

Table 2 shows the classification criteria used to distinguish on-farm irrigation reservoirs from non-elevated, man-made waterbodies such as ponds and borrow pits in the Mississippi Alluvial Plain (MAP).

For reference, model outputs are compared to waterbodies identified by the Cropland Data Layer (CDL; USDA-NASS, 2019) and the National Hydrography Dataset (NHD; USGS, 2019). The CDL and NHD are generally authoritative datasets which have water classes and features, but our comparisons with NAIP imagery, Google Earth imagery, the imagery base map from ArcGIS online, and our model output reveal that these datasets are not fit for assessment of our findings in our study area. The methods used to generate these datasets do not show a large number of the reservoirs found by our model and appear to show a number of flooded fields as bodies of water. Therefore, we feel that they do not merit inclusion in the results. We suspect there is a minimum area threshold for

NHD, and for both datasets, they could be effects from turbidity in combination with vegetation and seasonal variability in water level that mask reservoirs from being classified as water in these two datasets. We come to believe that they are just not intended for the purpose we wanted to use them for. Since they are not created in a manner that makes them useful as an assessment of irrigation reservoirs, the results of these comparisons are given in the supplemental materials document (Table A-1 and Table A-2) and shared as layers in the supplemental ArcGIS project folder (.zip) which is shared with this article.

Assessment of Model Identified Reservoirs

An assessment was performed on the model identified reservoirs using the most recently available "Imagery" basemap via ArcGIS Online Webmap (Esri, 2023). It was observed that this dataset is <1 m spatial resolution in our study area, which make it higher resolution than the 1 m NAIP data used in the model. Sample points were stratified across three classes based on the model outputs. These classes were "not water," "water," and "reservoir." Where not water was the area not found to be water within the study area, water was the area found to be water by the model in step one of the model and reservoirs are all compact bodies of water that were larger than the minimum threshold of 0.4 ha and raised above the surrounding land. This included Class 1 and Class 2 (Table 2) waterbodies. Each of these three classes were assessed with 100 points each.

RESULTS

Comparison of NIR to NDWI Method of Finding Water

Using the NDWI method of finding water results in a much lower number of waterbodies than the NIR method (Table 3). These results validate the selection of the NIR method of water classification from the 2019 NAIP imagery. However, the tools for choosing the method (if the user wants) are still available in the model which is shared along with the supplemental ArcGIS Pro project folder (.zip). This is done for the eventuality that they perform well in other regions or with other aerial imagery sources or imagery collected in different seasons.

Table 3. Comparison of waterbodies found using NIR method vs. NDWI method

Classification	Value	Number of Waterbodies (NIR)	Number of Waterbodies (NDWI)
Not Compact	Null	2,929	1,181
Not Raised	0	773	419
0 < Raised < 1 m	1	408	248
Raised > 1 m	2	199	137
Total Number of Waterbodies	N/A	4,309	1,985

A comparison of using the "NIR only" method versus the NDWI method was conducted for a portion of the study area to evaluate how the two methods compare. NIR captured over double the amount of water features compared to the NDWI method (See Table 3). Both models use the 15% threshold values for water features (NIR = 0–40, NDWI = 0.70–1).

Reservoir Detection in the CRCGA and GPCGA Study Areas

Once the necessary spatial data were compiled, less than one hour of laptop computing time was required to locate a total of 3,527 on-farm irrigation reservoirs in a 2.38-Mha study area made up of the CRCGA, GPCGA, and the Non-CGA area from Figure 2 (see Table 5). These reservoirs were estimated to have a combined surface area of 15,864 ha for the CRCGA, GPCGA, and Non-CGA areas combined (see Table 5). Note that these reservoir counts and surface areas in the CRCGA and GPCGA are larger than that of Yaeger et al. (2017) because the present study (a) encompasses a larger study area and (b) identifies any additional reservoirs constructed after the 2015 end-point of the Yaeger et al. (2017) study.

Table 4 is a summary table of area (ha) resulting from the model steps in the study area. The area changed at four different model steps: 1, 2, 3, and 7 (see supplemental materials for technical descriptions of all model steps). Step 1 is defining the study area; Step 2 is classifying landcover as water/land; Step 3 is discarding water polygons < 0.4 ha; Step 7 is filtering water by elevation class resulting in two classes of raised waterbodies representing potential reservoirs. The percentage represents the ratio of water:land comparing the water resulting from each step to the area of land from Step 2.

Table 4. Surface areas (ha) resulting from each model step

	Study Area		
Step 1	2,384,109		
	Water	**Land**	**Water:Land**
Step 2	267,167	2,116,942	12.62%
	Compact Waterbodies		**Water:Land**
Step 3	64,866		3.06%
	Reservoirs		**Water:Land**
Step 7	15,864		0.75%

Table 5. Surface areas and counts of model-identified irrigation reservoirs

Study Area	Reservoir Class[a]	Reservoir Count	Water Surface Area (ha)
CRCGA	1	432	1,333
	2	209	1,821
	1 & 2	641	3,154
GPCGA	1	1,509	4,908
	2	1,100	6,966
	1 & 2	2,609	11,874
Non-CGA	1	214	654
	2	63	182
	1 & 2	277	836

[a]SeeTable 2 for reservoir elevation classes.

Table 5 represents the numbers and water surface areas of model-identified irrigation reservoirs in the CRCGA, the GPCGA, and the Non-CGA, as of July 2019.

MODEL VALIDATION AND ACCURACY ASSESSMENT

The assessment of the model accuracy results in a producer's accuracy for a given class representing the proportion of pixels that were classified correctly (2). The producer's accuracy for not water is 99%; for non-reservoir water is 87%; and for reservoirs is 60%. The errors in producer's accuracy are known as errors of omission or Type 2 errors, which for not water is 1%; for non-reservoir water is 13%; and for reservoirs is 40%. The user's accuracy for a given class represents the proportion of pixels identified on the map as being in that class that are actually in that class on the ground (3). The user's accuracy for not water is 88%; for non-reservoir water is 68%; and for reservoirs is 100%. The errors in user's accuracy are known as errors of commission or Type 1 errors, which for not water is 12%; for non-reservoir water is 38%; and for reservoirs is 0%. The overall accuracy takes the sums of the correctly identified pixels in all classes, divided by the number of sample points (4). The overall accuracy across these three classes is 82%. The Kappa coefficient evaluates how well the classification performs as compared to random, ranging from -1 to 1; a negative value indicates the classification is worse than random, a value of zero would be the same as random, and a positive value indicates that the classification is better than random (5). The Kappa coefficient is 0.73. See Table 6 for the Confusion Matrix of the assessment.

$$Producer's\,Accuracy_{class\,x} = \frac{n\,correctly\,classified\,pixels_{class\,x}}{column\,total} \tag{2}$$

$$User's\,Accuracy_{class\,x} = \frac{n\,correctly\,classified\,pixels_{class\,x}}{row\,total} \tag{3}$$

$$Overall\,Accuracy = \frac{correctly\,classified\,pixels}{n\,of\,sample\,points} \tag{4}$$

$$Kappa = \frac{\left(n\,of\,sample\,points\ *n\,of\,corrrectly\,classified\,pixels\right) - \left(sum\,of\,row\,totals * column\,totals\right)}{\left(n\,of\,sample\,points^2\right) - \left(sum\,of\,row\,totals * column\,totals\right)} \tag{5}$$

Table 6 represents the Accuracy Assessment Confusion Matrix, where N = not water, W = water but not reservoirs, and R = reservoirs. The table includes Producer's and User's Accuracy for each class, Overall Accuracy, and Kappa. The reference data is NAIP 2019.

This assessment affirms that irrigation reservoirs are most likely to be found using this method as long as the model is accompanied by recent elevation data. Of the sample points representing errors of commission, all false reservoir detections were instead aquaculture ponds that were raised above the surrounding area. Furthermore, of the sample points representing errors of omission, and therefore not identified by the model, all are "false negative" omissions due either to the presence of excess turbidity (Figure 5-A) or vegetation growing inside of the reservoir (Figure 5-B). Figure 6 illustrates examples of four different classes of reservoirs found by the model. These include waterbodies that

Table 6. Accuracy assessment confusion matrix

		Reference Data					
		N	**W**	**R**	**row totals**	**User's Accuracy**	
Classified data	N	99	13	0	112	88%	
	W	1	87	40	128	68%	
	R	0	0	60	60	100%	
	column totals	100	100	100			
	Producer's Accuracy	99%	87%	60%		82.00%	Overall Accuracy
						0.73	Kappa

are not compact and compact waterbodies that are not raised (these represent the water class), compact waterbodies that are raised (but not more than one meter), and compact waterbodies that are raised more than one meter (these represent the reservoir class).

Figure 5 presents examples of (A) turbidity and (B) vegetation that interfere with NIR spectral reflectance, causing a 13% Type-II (false-negative) error rate in the automated detection of on-farm reservoirs, relative to a visually-curated dataset.

Figure 5. Examples of (A) turbidity and (B) vegetation interference

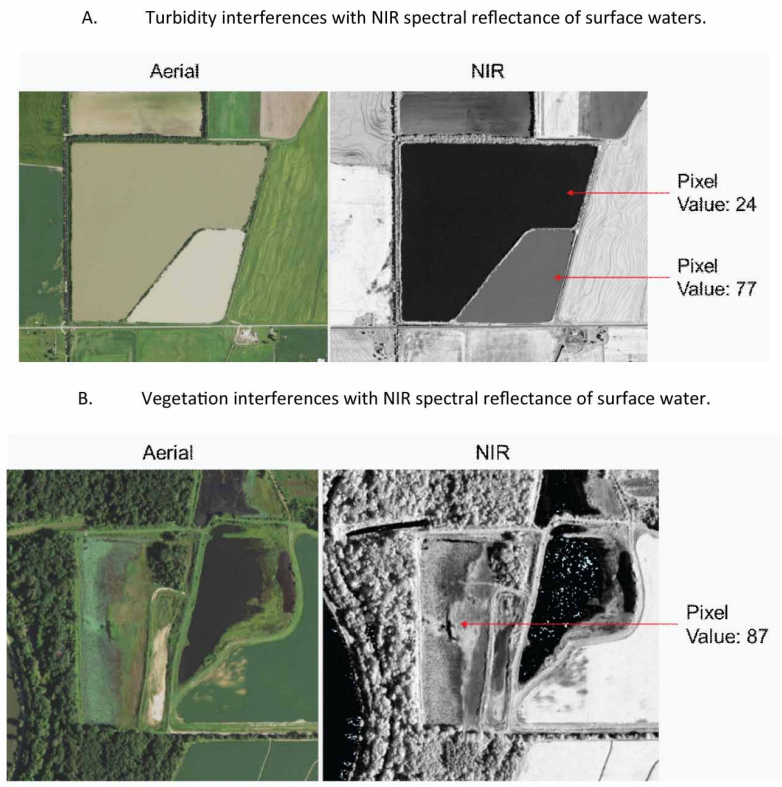

Figure 6 shows examples of the four waterbody types classified using an automated detection tool in a 2.38-Mha region of eastern Arkansas. The waterbodies were classified as "not compact" (blue), "compact but not raised" (green), "raised but less than 1-meter" (red), and "raised greater than 1-meter" (yellow). An on-farm irrigation reservoir, as defined by this project, is outlined in yellow.

Figure 6. Waterbody classifications

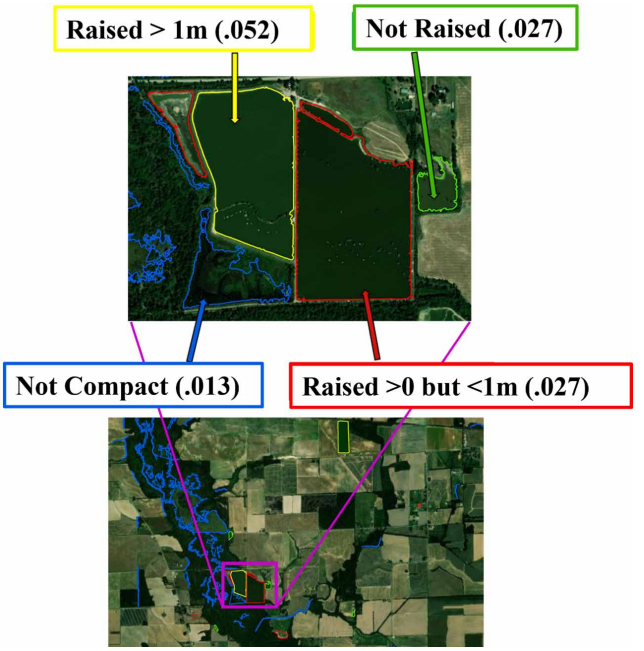

DISCUSSION

The assembly of a quick running model implementing a variety of methods to find waterbodies, to determine and discriminate between them on the basis of compactness, and to classify compact waterbodies on the basis of elevation above the surrounding terrain is successfully accomplished in the model produced by this research. An accuracy assessment of the model output illustrates errors in the model that provide a variety of potential improvements that might be carried out in the future. Many of these potential improvements relate to temporal considerations. This includes not only the temporal resolution of the aerial imagery and elevation surfaces needed for the model, but also the seasonality of aerial imagery and the gap in time between the collection of the aerial imagery and the elevation surface. Furthermore, the spatial extent within which the model is appropriate might be expanded if global datasets of satellite imagery and elevation surfaces of sufficient resolution can be implemented.

The temporal resolution of data needed to run the model is an important source of error in the model. Such problems arise when there is a mismatch in timing between the elevation dataset and the spectral dataset. For example, if the reservoir was built after the DEM acquisition date, the model cannot identify the waterbody as being raised. Wu et al. (2016) also note the temporal shift from NAIP to Landsat as a source of error, as they modeled flooding inundation areas in water filled depressions in Minnesota. One way that this could be addressed in future modeling is by using multi-spectral imagery from a source that allows date matching to the elevation data source(s) collected at close to

the same time. More practically, the aerial imagery can be slightly older than the elevation source; then, reservoirs in the imagery would be present in the elevation dataset. Error associated with the temporal problem might be acceptable in regions building an initial dataset, as subsequent updates would resolve over time. Another potential improvement might be choosing imagery dates in the spring. This is before irrigation occurs when reservoirs should be filled with winter precipitation. Early spring imagery could reduce the temporal error from NAIP which is collected mid-growing season when irrigation is occurring and vegetation in the reservoirs is leafed out.

While the imagery frequency is somewhat easily overcome (as mentioned above), the same is not true for elevation data. The elevation datasets available across this study area were collected from 2011 to 2017. This indicates a low re-issue cycle for this type of data and will be the inherent temporal limitation for the model. This low temporal resolution for elevation data represents the primary limitation of this model. This also means that the optimal time to conduct reservoir inventories is set by the generation of updated elevation data.

With the proliferation of spaceborne high spatial resolution ($\leq$ 1 m) collection platforms there is wide availability of multi-spectral imagery. The value of using elevation with multi-spectral imagery is revealed by this model, and effort should be made to further develop the means to collect $\leq$ 1-m DEMs on a shorter time cycle. In the US, this suggests a good reason for collecting LiDAR for 3DEP with NAIP—or at least, updating 3DEP on a similar timeframe to NAIP, such as every two to three years. In space, it might mean improving the Earth observation satellites with higher resolution elevation collection capabilities. Nonetheless, the model can still be used for surface water assessments in any region with high-resolution NIR imagery and high-resolution DEMs with the understanding that the relative dates of the imagery and DEM will limit the timeframe of reservoir assessment.

Because the study area is also home to aquaculture, errors associated with identification of fishponds as reservoirs were anticipated. This proved to be a significant source of error (40% of our errors of omission for the reservoir class), especially in the GPCGA. Turning the error into a positive characteristic, the model could be used to conduct aquacultural pond inventories for both reservoirs and the portion of fishponds that are raised above the surrounding terrain. If the model were repurposed in this way, it is possible the errors of omission for the reservoir class would have been zero. The overall model accuracy of 82% is pretty good, especially when considering that 100% of the reservoir class errors of omission are because the model identified elevated fishponds as reservoirs. This can almost be accepted as a non-error since the model was not designed to discriminate between types of raised man-made waterbodies. Unfortunately, the model did not find all fishponds, as noted from a number of non-raised waterbodies which are known to be fishponds by the authors. So, it seems dubious to repurpose the model to find reservoirs and only raised fishponds, but it would work, and the accuracy would dramatically improve. Future improvements to the model should consider this purpose.

The 'Localized Elevation' technique used in the model is only expected to be helpful for low relief regions, such as the MAP and other relatively flat alluvial plains worldwide. In an area of higher relief, on-farm reservoirs are typically constructed across small portions of upland watersheds where an earthen dam traps the water (NRCS, 2018). It may be possible to adjust the model to find such waterbodies by making modifications to the buffer rings and the statistics used to compare them.

While Mondejar and Tongco (2019) found the NIR threshold method outperformed other water finding indices, as did we, this technique of using the NIR band (Figure 5) alone for surface water detection might be inferior to other water detection methods. Notable among such indices is the NDWI ((1); Gao, 1996), which might perform better than NIR along other study regions with imagery collected in different seasons or with imagery collected with platforms other than NAIP. In the cases of the watersheds presented in this paper, the "NIR only" (aka NIR-threshold) method of running the model was more successful than the NDWI method. It should be noted, however, that both methods require the choice of a threshold when classifying waterbodies. Because of the data type differences between an eight-bit integer (0-255) with the "NIR only" method and a floating-point value of $\pm$1

with the NDWI method, it is possible that the author's *ad hoc* means of choosing that threshold were not equivalent between the methods.

Future improvements to these techniques must involve choosing better aerial imagery sources and investigating calibration of the method of water identification. This relates to the data source and either of the two methods tested, the NAIP-NDWI or NAIP-NIR only methods. The differences seen between these two water identification methods in the first step of the model could be due to many factors including vegetation or algal blooms in the water, suspended sediments, or a combination of these two and other unknown factors that are particular to the time the imagery was collected. Chen et al. (2022) review remote sensing papers related to assessing remote sensing techniques for inland water quality. They summarize from this meta-analysis that remotely sensed imagery of inland waterbodies, in general, have low accuracy because of multiple factors. The research they reviewed corroborated our findings in that the nature of turbidity related to concentrations of chlorophyll-a, suspended particulate matter, and colored dissolved organic matter. Of course, the clorophyll-a they are observing is often algae, and sometimes our error was related to the leaf area of vegetation growing in the reservoir. These sources of error are further corroborated by Yigit et al. (2019) who characterize water in the Borabey Lake area in Eskisehir, Turkey for water quality using RapidEye Satellite imagery. Other than finding fishponds, we found that the largest portion of the error in our model is differentiating water from soil or vegetation because of turbidity or plants growing in the reservoirs. For these reasons, testing different water identification techniques combined with better data would certainly be two future streams of inquiry that hold promise for improving accuracy.

The water identifies on the aerial imagery raster by the model results in a polygon representing the waterbody boundary. Some of the waterbodies in eastern Arkansas contain vegetation. When there is an existing vegetation layer on the waterbody, the model will not identify water, or, in some cases, the model will identify the waterbody but will miscalculate the area depending on how much of the waterbody is covered in vegetation and/or is high in turbidity. We suspect that this error in identifying waterbody boundaries contributes to errors in waterbody area, count, and in the accuracy assessment (Tables 4, 5, and 6 – Waterbody Areas, Counts and the Assessment Confusion Matrix).

"Leaf-off" imagery collection takes place in the cooler and wetter part of the year in this study area. Therefore, using "leaf-off" imagery might be superior to "leaf-on" imagery, suggesting that NAIP is not the optimal aerial imagery for water detection. This is partly because of the vegetation blocking the water in the growing season when NAIP is collected. This is also because some reservoirs may be at lower levels in this period because they are being used for irrigation. The reduced depth of water in the reservoir not only contributes to an increase in vegetative growth in low-water and empty reservoirs but also changes the position of the shoreline along the reservoir levee. These factors suggest using "leaf-off" imagery collected in the spring, when reservoirs are full, would likely improve the model accuracy.

Based on a report by Shelby Johnson, the Director of the Arkansas GIS Office (Arkansas GIS Board - 3rd Quarterly Meeting, 2023), we anticipate two updates to datasets that might dramatically improve the success rate of this model. The first is a 0.228-m resolution, leaf-off aerial multi-spectral (RGB and NIR) imagery dataset collected for the entire state of Arkansas in the winter of 2022-2023 (ADOP, 2023). This dataset is currently being processed and is expected to be completed and released in early 2024. The second dataset is an anticipated 0.5-m LiDAR-based elevation collection funded by the USDA-NRCS to update the 3DEP elevation dataset. Funding is in place, and the plan is to collect the entire lowland portion of eastern Arkansas in the leaf-off period of the winter of 2023-2024. Upon the availability of these two datasets, the leaf-off aerial imagery and the new sub-meter LiDAR-based DEM could directly be used by this model to produce an up-to-date reservoir inventory for eastern Arkansas. The update period of these datasets (especially elevation) should drive future reservoir inventory efforts in the region.

Finally, it is expected that, with slight modifications to the buffer zones, this model should be able to utilize Sentinel 2 multi-spectral satellite imagery (20- to 30-m spatial resolution) to better

identify water than the NIR collected aerially. Moreover, Sentinel 2 has shortwave infrared bands which might be able to identify turbid water and vegetated waterbodies better than the current aerial method. The expected difficulty with this method is the availability of a timely global 10- to 20-m elevation dataset which could be used to assess waterbody elevation. If this elevation layer can be located, and the model calibrated for this lower resolution, our model should work worldwide to find raised bodies of water in otherwise low relief environments.

Additional future work might use the spectral characteristics of these reservoirs in a way that allows for the identification of more turbid water. When considering the limitations presented by the spectral effects of suspended sediment in waterbodies, this seems to be a major limitation for identification. It is possible that, without incorporating uncommonly available shortwave infrared bands in the analysis, this is just not possible with the currently available data. Using lower resolution Sentinel 2 imagery might address this as long as the 20-meter resolution allows for reasonable reservoir boundary characterization.

CONCLUSION

The critical groundwater regions of eastern Arkansas are important for their diverse agricultural production. The proliferation of irrigation reservoirs has complicated the efforts to conjunctively manage the region's water resources. One critical component of managing regional surface water is a proper inventory of irrigation reservoirs. Before this paper, there was a single inventory in the study region produced in 2017 by Yaeger et al. from 2015 NAIP imagery. Notably, the visually curated methods used to generate this dataset were time intensive, and even though the dataset is only six years old, it is already in need of updating.

The novel contribution to the literature supplied by this research is the automation of a collection of practical remote sensing and GIS based methods into an ArcGIS Pro based model. The model produced by this research was able to find 3,527 irrigation reservoirs within a 2.38-Mha area in less than an hour using an off-the-shelf laptop. The benefit of this model over the methods employed by Yeager et al (2017) is that this model is fast at finding reservoirs (and apparently raised fishponds) and can be reused once new aerial imagery and elevation data are generated.

While its overall accuracy of 82% may not seem great, it should be noted that 13.2% of the overall error is related to false-positive detections of raised fishponds as reservoirs. So, if the purpose of the model is adjusted to finding reservoirs and raised fishponds and this error is removed, the overall accuracy would rise to 95%. Based on these reasons, we can say we met our objectives. This model fills the gap now, by updating the existing reservoir inventory and provides means for keeping such gaps filled in the future by creating a model to automate this process. The resulting inventory and set of methods for keeping it up to date are necessary precursors to ongoing effective conjunctive water management, especially for regions needing to develop surface water resources to offset groundwater declines.

The model is useful for accurately identifying on-farm reservoirs (and raised fishponds) in eastern Arkansas. This approach and this tool should be useful across the broader MAP and other low-relief alluvial environments. Such inventories are important components for future reservoir establishment and site selection. Moreover, consideration of a region's current and future potential reservoirs will improve groundwater modeling efforts aimed at predicting local variations in groundwater levels over time.

AUTHOR'S NOTE

An ArcGIS Pro project folder with our model, our results and the Yaeger er al (2017) boundaries and Shults et al (2024) establishment dates have been made available at Shults, Daniel D.; Nowlin, John W.; Massey, Joseph H.; Reba, Michele L. (2024). Data from: Automated Detection of On-Farm

Irrigation Reservoirs: A Necessary Precursor for Conjunctive Water Management in Two Critical Groundwater Regions of Arkansas. Ag Data Commons. Dataset. https://doi.org/10.15482/USDA.ADC/24851661.v1. These materials are described in the included supplemental documentation.

The authors declare there is no conflict of interest.

This work was supported by the University of Arkansas System, Division of Agriculture: Arkansas State University Research Unit (XASU) through the Resilient Agricultural Systems in the Arkansas Delta (RASAD) funding opportunity. Funding was also made available through two cooperative agreements with the U.S. Department of Agriculture - Agricultural Research Service, first with Delta Water Management Research Unit (Agreement No. 58-6024-1-005) and second with Sustainable Water Management Research Unit (Agreement No. 58-6066-1-041).

REFERENCES

Alexandridis, T. K., Zalidis, G. C., & Silleos, N. G. (2008). Mapping irrigated area in Mediterranean basins using low cost satellite Earth Observation. *Computers and Electronics in Agriculture*, *64*(2), 93–103. doi:10.1016/j.compag.2008.04.001

Arkansas, G. I. S. (2023). *Arkansas GIS Users Forum Biennial Symposium, Jonesboro Arkansas* (Officiated by Shelby Johnson, Director of the Arkansas GIS Office). Arkansas GIS. https://www.transform.ar.gov/gis-office/gis-board/

Arkansas Digital Ortho Program (ADOP). (2023). *Arkansas Department of Transformation and Shared Services*. ADOP. https://www.transform.ar.gov/gis-office/programs/arkansas-digital-ortho-program-adop/

Arkansas Groundwater Protection and Management Report for 2015. (2016). Arkansas Natural Resources Commission (ANRC). (pp. 1–81). ANRC. https://www.agriculture.arkansas.gov/natural-resources/news/annual-reports/

Arkansas Natural Resources Commission (ANRC), (2017). 2017 Annual Report. 1–32. https://www.agriculture.arkansas.gov/wp-content/uploads/2022/06/AnnualReport_FY2017_FINAL.pdf

Arkansas Natural Resources Commission (ANRC), (2019). Critical Groundwater Areas. https://www.agriculture.arkansas.gov/wp-content/uploads/2020/05/Critical_Areas_2019.pdf

Bakuła, K., Pilarska, M., Salach, A., & Kurczyński, Z. (2020). Detection of levee damage based on UAS data—Optical imagery and LiDAR Point Clouds. *ISPRS International Journal of Geo-Information*, *9*(4), 248. doi:10.3390/ijgi9040248

Bedinger, M. S., & Jeffery, H. G. (1964). Ground water in the lower Arkansas River Valley, Arkansas. In Water Supply Paper (1669–V; Water Supply Paper). United States Government Publishing Office (USGPO). doi:10.3133/wsp1669V

Chen, J., Chen, S., Fu, R., Li, D., Jiang, H., Wang, C., Peng, Y., Jia, K., & Hicks, B. J. (2022). Remote sensing big data for water environment monitoring: Current status, challenges, and future prospects. *Earth's Future, 10*(2), e2021EF002289. 10.1029/2021EF002289

Clark, B., Hart, R., & Gurdak, J. (2011). USGS Professional Paper 1785: Groundwater Availability of the Mississippi Embayment (Professional Paper 1785). https://pubs.usgs.gov/pp/1785/

Clark, B. R., Westerman, D. A., & Fugitt, D. T. (2013). Enhancements to the Mississippi Embayment Regional Aquifer Study (MERAS) groundwater-flow model and simulations of sustainable water-level scenarios. *Scientific Investigations Report*, (2013–5161). 10.3133/sir20135161

Clemmens, A. J., Anderson, S. S., & U.S. Committee on Irrigation and Drainage (Eds.). (2003). Water for a sustainable world -- limited supplies and expanding demand. *Second International Conference on Irrigation and Drainage*. U.S. Committee on Irrigation and Drainage. https://www.ars.usda.gov/ARSUserFiles/53442000/AnnualReports/AnnualReport2003/2003AnnualReport.pdf

Czarnecki, P., Omer, A. R., & Dyer, J. (2024). Quantifying Capture and Use of Tailwater Recovery Systems. *Journal of Irrigation and Drainage Engineering*, *143*(1), 05016010. Advance online publication. doi:10.1061/(ASCE)IR.1943-4774.0001124

DeVantier, B. A., & Feldman, A. D. (1993). Review of GIS Applications in Hydrologic Modeling. *Journal of Water Resources Planning and Management*, *119*(2), 246–261. doi:10.1061/(ASCE)0733-9496(1993)119:2(246)

Ecology and Environment, INC (E&E INC). (2011). *Recommendations for a Statewide Ground Water Management Plan (DNR Contract No. 2215-10-04; pp. 1–512).* Office of Conservation, Louisiana Department of Natural Resources. https://www.dnr.louisiana.gov/assets/OC/env_div/gw_res/20111206_GWPLAN_FINALTECHAPP.pdf

Evett, S., Carman, D., & Bucks, D. (2003). *Expansion of Irrigation in the Mid South United States*: *Water Allocation and Research Issues*. ARS. https://www.ars.usda.gov/research/publications/publication/?seqNo115=144302

Feyisa, G. L., Meilby, H., Fensholt, R., & Proud, S. R. (2014). Automated Water Extraction Index: A new technique for surface water mapping using Landsat imagery. *Remote Sensing of Environment*, *140*, 23–35. doi:10.1016/j.rse.2013.08.029

Gao, B. (1996). NDWI—A normalized difference water index for remote sensing of vegetation liquid water from space. *Remote Sensing of Environment*, *58*(3), 257–266. doi:10.1016/S0034-4257(96)00067-3

Hartvich, F., & Jedlička, J. (2019). Progressive increase of inputs in floodplain delineation based on the DEM: Application and evaluation of the model in the catchment of the Opava river. *Auc Geographica*, *43*(1), 87–104. doi:10.14712/23361980.2015.74

Ji, L., Zhang, L., & Wylie, B. (2009). Analysis of dynamic thresholds for the normalized difference water index. *Photogrammetric Engineering and Remote Sensing*, *75*(11), 1307–1317. doi:10.14358/PERS.75.11.1307

Khan, S. N., Mujahid, D., & Zahid, S. M. H. (2022). Application of GIS/RS in assessment of flash flood causes and damages: A case study of Budhni Nullah, District Peshawar, Khyber Pakhtunkhwa, Pakistan. *Sustainable Business and Society in Emerging Economies, 4*(2), 283–294. https://publishing.globalcsrc.org/ojs/index.php/sbsee/article/view/2262

King, S. E. (2021). *A Study of Adoption and Costs of NRCS Avoid, Control, and Trap*. Agricultural Conservation Practices in Arkansas. [M.S., Arkansas State University], https://www.proquest.com/docview/2565083303/abstract/82EF9A33423F4FC8PQ/1

Kovacs, K., Xu, Y., West, G., & Popp, M. (2016). The tradeoffs between market returns from agricultural crops and non-market ecosystem service benefits on an irrigated agricultural landscape in the presence of groundwater overdraft. *Water (Basel)*, *8*(11), 501. doi:10.3390/w8110501

Kresse, T. M., Hays, P. D., Merriman, K. R., Gillip, J. A., Fugitt, D. T., Spellman, J. L., Nottmeier, A. M., Westerman, D. A., Blackstock, J. M., & Battreal, J. L. (2014). Aquifers of Arkansas: Protection, management, and hydrologic and geochemical characteristics of groundwater resources in Arkansas. *U.S. Geological Survey Scientific Investigations Report*, 2014–5149. doi:10.3133/sir20145149

Leslie, D. L., Reba, M. L., Godwin, I. A., & Yaeger, M. A. (2022). Groundwater trends during 1985 to 2019 in a critical groundwater area of northeastern Arkansas. *Journal of Soil and Water Conservation*, *77*(1), 67–77. doi:10.2489/jswc.2022.00170

McFeeters, S. K. (1996). The use of the normalized difference water index (NDWI) in the delineation of open water features. *International Journal of Remote Sensing*, *17*(7), 1425–1432. doi:10.1080/01431169608948714

Missouri Water Resources Plan, Update 2020. (2020). Missouri Department of Natural Resources (MDNR). https://dnr.mo.gov/document-search/missouri-water-resources-plan-update-2020

Mondejar, J. P., & Tongco, A. F. (2019). Near infrared band of Landsat 8 as water index: A case study around Cordova and Lapu-Lapu City, Cebu, Philippines. *Sustainable Environment Research*, *29*(1), 16. doi:10.1186/s42834-019-0016-5

A W. P. (2014). (AWP) 2014 Update Summary. Arkansas Natural Resources Commission (ANRC). (pp. 1–16). https://www.agriculture.arkansas.gov/natural-resources/divisions/water-management/arkansas-water-plan/arkansas-water-plan-2014/arkansas-water-plan-2014-update-summary/

Preusch, D. P., & Rezakhani, M. (1999). Integrating Geographic Information Systems (GIS) and Watershed Modeling. *WRPMD'99: Preparing for the 21st Century*, (pp. 1–10). ASCC. 10.1061/40430(1999)154

Rodrigues, L. N., Sano, E. E., Steenhuis, T. S., & Passo, D. P. (2012). Estimation of Small Reservoir Storage Capacities with Remote Sensing in the Brazilian Savannah Region. *Water Resources Management*, *26*(4), 873–882. doi:10.1007/s11269-011-9941-8

Shults, D. D. (2021). *Spatial-Temporal Modeling of Agricultural Water Surface Features in Northeastern Arkansas* [M.S.A., Arkansas State University]. https://www.proquest.com/docview/2597849407/abstract/80C3C94060F446D6PQ/1

Shults, D. D., Reba, M. H., Nowlin, J., Massey, J., & Read, Q. (2023). Use of low-resolution imagery and presence–absence analysis to establish irrigation reservoir histories for improved groundwater modeling and conjunctive water management in two Arkansas critical groundwater areas. *Agricultural Water Management*, 108678.

Singh, A., Panda, S. N., Saxena, C. K., Verma, C. L., Uzokwe, V. N. E., Krause, P., & Gupta, S. K. (2016). Optimization Modeling for Conjunctive Use Planning of Surface Water and Groundwater for Irrigation. *Journal of Irrigation and Drainage Engineering*, *142*(3), 04015060. doi:10.1061/(ASCE)IR.1943-4774.0000977

Tucker, C. J. (1979). Red and photographic infrared linear combinations for monitoring vegetation. *Remote Sensing of Environment*, *8*(2), 127–150. doi:10.1016/0034-4257(79)90013-0

United States Army Corps of Engineers. (2006). *Grand Prairie Region and Bayou Meto Basin, Arkansas Project: Bayou Meto Basin, Arkansas, General Reevaluation Report.* United States. Army. Corps of Engineers. Memphis District. https://hdl.handle.net/11681/36360

U.S. Army Corps of Engineers (USACE). (1999). Eastern Arkansas Region Comprehensive Study: Grand Prairie Region and Bayou Meto Basin, Arkansas Project, Grand Prairie Project, *General Re-Evaluation Report. U.S. Army Corps of Engineers*. https://www.mvm.usace.army.mil/Portals/51/docs/missions/projects/Grand%20Prairie%20Area%20Demonstration%20Project/General%20Reevaluation%20Report/General_Reevaluation_VI.pdf

U.S. Department of Agriculture-National Agricultural Statistics Service (USDA-NASS). (2019). *National Agricultural Statistics Service - Research and Science - CropScape and Cropland Data Layers.* USDA. https://data.nal.usda.gov/dataset/cropscape-cropland-data-layer

U.S. Department of Agriculture-Natural Resource Conservation Service (USDA-NRCS). (2018). Conservation Practice Standard: Pond. *NRCS Arkansas: Code 378-1.* eFotg. https://efotg.sc.egov.usda.gov/api/CPSFile/9902/378_AR_CPS_Pond_2018

U.S. Department of Agriculture-Natural Resource Conservation Service (USDA-NRCS) (2019). *2004-2018 ProTracts Program Contracts System Data in Addition to the National Planning and Agreements Database Data*.

U.S. Geological Survey (USGS). (2011). *3D Elevation Program*. USGS. https://www.usgs.gov/core-science-systems/ngp/3dep

Vories, E. D., & Evett, S. R. (2014). Irrigation challenges in the sub-humid US Mid-South. *International Journal of Water*, *8*(3), 259–274. doi:10.1504/IJW.2014.064220

Wu, Q., Deng, C., & Chen, Z. (2016). Automated delineation of karst sinkholes from LiDAR-derived digital elevation models. *Geomorphology*, *266*, 1–10. doi:10.1016/j.geomorph.2016.05.006

Wu, Q., Lane, C. R., Li, X., Zhao, K., Zhou, Y., Clinton, N., DeVries, B., Golden, H. E., & Lang, M. W. (2019). Integrating LiDAR data and multi-temporal aerial imagery to map wetland inundation dynamics using Google Earth Engine. *Remote Sensing of Environment*, *228*, 1–13. doi:10.1016/j.rse.2019.04.015 PMID:33776151

Yaeger, M. A., Massey, J. H., Reba, M. L., & Adviento-Borbe, M. A. A. (2018). Trends in the construction of on-farm irrigation reservoirs in response to aquifer decline in eastern Arkansas: Implications for conjunctive water resource management. *Agricultural Water Management*, *208*, 373–383. doi:10.1016/j.agwat.2018.06.040

Yaeger, M. A., Reba, M. L., Massey, J. H., & Adviento-Borbe, M. A. A. (2017). On-Farm irrigation reservoirs in two Arkansas critical groundwater regions: A comparative inventory. *Applied Engineering in Agriculture*, *33*(6), 869–878. doi:10.13031/aea.12352

Yazoo Mississippi Delta Joint Water Management District (YMD). (2006). *Yazoo Mississippi Delta Joint Water District Water Management Plan*. YMD. https://www.ymd.org/ymd-water-management-plan

Yigit Avdan, Z., Kaplan, G., Goncu, S., & Avdan, U. (2019). Monitoring the water quality of small water bodies using high-resolution remote sensing data. *ISPRS International Journal of Geo-Information*, *8*(12), 12. Advance online publication. doi:10.3390/ijgi8120553

Zhang, C., Zhang, H., & Zhang, L. (2021). Spatial domain bridge transfer: An automated paddy rice mapping method with no training data required and decreased image inputs for the large cloudy area. *Computers and Electronics in Agriculture*, *181*, 105978. doi:10.1016/j.compag.2020.105978

Daniel Shults, is a geospatial technologist specializing in precision agriculture. He has worked in both the agricultural equipment industry and at the USDA-NRCS. He graduated from the Arkansas State University College of Agriculture with a Bachelor's in Ag. Studies with an emphasis in Agricultural Systems Technology, this was followed by a Master's of Science in Agriculture with the Digital Agriculture Concentration. Daniel's specializations revolve around applying GIS and drones to solve environmental problems related to irrigation and agricultural surface water infrastructure.

John W. Nowlin, a geographer, is an Assistant Professor of Geospatial Technology in the College of Agriculture at Arkansas State University; he teaches GIS and regenerative agriculture classes in the GIS and Precision Agriculture program. His research specializations include human-environment interactions, niche agricultural suitability, viticultural site selection, terroir analysis, and micro-topographic analysis using remotely sensed spatial data collected in-situ, from drone, aerial and satellite remote sensing. He uses GIS based topographic, climate, and soil raster surfaces for environmental modeling, including research related to cotton, rice, and irrigation utilizing applications of precision elevation.

Joseph Massey, PhD, is a research agronomist with the Delta Water Management Research Unit of the USDA Agricultural Research Service located in Jonesboro, Arkansas, USA. His research seeks to address agricultural water management issues to help with current and future resource availability.

Michele L. Reba is a research hydrologist, lead scientist, and acting research leader at the USDA-ARS-Delta Water Management Research Unit in Jonesboro, AR. The mission of the unit is to execute research related to agricultural water resources management at the multiple scales to further our knowledge base, evaluate technological solutions and inform crop production practices. In addition to her current research in the US Mid-South, she has studied water resources issues in the western United States, the Dominican Republic, Haiti, and Antarctica. Dr. Reba has received national awards for her research related to sustainability, rice research, and irrigation.